GRAVITATIONAL LENSING

Sjur Refsdal[1] and **Jean Surdej**[2,*]

[1]Hamburg Observatory, Gojenbergsweg 112, $D-2050$ Hamburg 80, Germany

[2]Institut d'Astrophysique, Avenue de Cointe 5, $B-4000$ Liège, Belgium

*Maître de Recherches au FNRS (Belgium)

ABSTRACT. Atmospheric lensing effects deform our view of distant objects; similarly, without any doubt, gravitational lensing perturbs our view of the distant Universe and affects our physical understanding of various classes of extragalactic objects. We summarize here part of the theoretical and observational evidences supporting these claims.

After briefly reviewing the history of gravitational lenses, we recall the basic principles underlying the formation of gravitationally lensed images of distant cosmic sources. We describe a simple optical lens experiment, which was actually shown during the oral discourse, and which accounts for all types of presently known gravitational lens systems.

The various optical and radio searches for new gravitational lens systems that are being carried out at major observatories are reviewed. State-of-the-art observations of selected gravitational lens systems, obtained with highly performing ground-based telescopes, are then presented. These include several examples of multiply imaged QSO images, radio rings and giant luminous arcs.

Through the modeling of these enigmatic objects, we show how it is possible to weigh the mass of distant lensing galaxies as well as to probe the distribution of luminous and dark matter in the Universe. Among the astrophysical and cosmological interests of observing and studying gravitational lenses, we also discuss the possibility of deriving the value of the Hubble parameter H_o from the measurement of a time delay, and how to determine the size and structure of distant quasars via the observational study of micro-lensing effects.

At the end of this paper, we conclude on how to possibly achieve major astrophysical and cosmological goals in the near future by dedicating, on a site with good atmospheric seeing conditions, a medium size (2-3 m) telescope to the photometric monitoring of the multiple images of known and suspected gravitational lens systems.

J. Bergeron (ed.), Highlights of Astronomy, Vol. 9, 3–32.

1. INTRODUCTION

**"The human mind has first to construct forms,
independently before we can find them in things"
A. Einstein**

Approximately 12 years ago, the dream of several theoreticians who had anticipated the existence of gravitational lenses became reality: the first gravitational lens (GL) was serendipitously identified in the sky by Walsh, Carswell and Weymann (1979). Since then, several tens of additional lenses have been found and studied.

It has of course been a great pleasure for us to deliver an invited discourse on these fascinating objects during the XXIst General Assembly of the IAU in Buenos Aires. We have tried, in our discourse, to convince the audience that these objects should deserve more observational attention in the future as they turn out to be full of promises for astrophysical and cosmological applications. We present here a somewhat extended version of our talk.

The general layout of our paper is organized as follows: in order to set up some analogy with gravitational lensing, we discuss first the case of mirages formed by atmospheric "lensing" (Section 2). We then summarize the historical background of gravitational lenses (Section 3). The basic principles of gravitational lensing are briefly discussed afterwards (Section 4). By means of an optical lens experiment (Figure 5) as well as observations of known astronomical lensed objects (Section 5), we illustrate the major properties of gravitational lenses as they exist in the Universe. Finally, selected astrophysical and cosmological applications of gravitational lensing (Section 6) and some general conclusions are presented at the end of this article (Section 7).

Because of space limitation, we apologize for only covering a few subjectively selected aspects of gravitational lensing and also for not quoting the names of most astrophysicists who have contributed to the development of our knowledge in this field. They are just too numerous! A more detailed and complete approach will soon be available in a review paper by Blandford and Narayan (1992) and also in the book of Schneider, Ehlers and Falco (1992).

2. ATMOSPHERIC LENSING

Figure 1 gives a schematic representation of the light rays from a distant source when the ground turns out to be somewhat hotter than the ambient air. Because air refraction always leads to a bending of light rays towards regions of colder air, the formation of one lower, inverted and somewhat deformed image of a distant source may result. The right side of Fig. 1 illustrates such a double image: a distant car as photographed along the North Panamericana highway between the towns of Pichidangui and La Serena, in Chile.
Such atmospheric mirages, usually consisting of two single images, can actually be seen

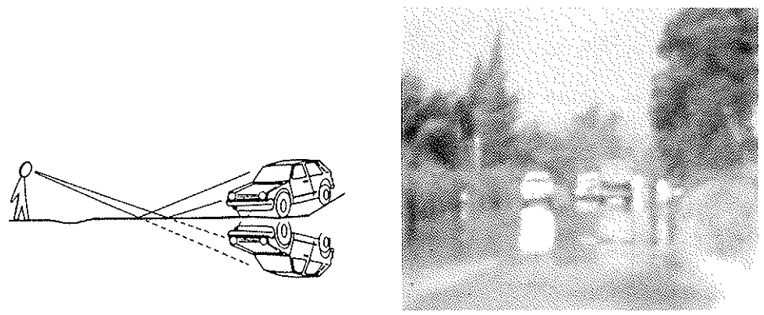

Figure 1: Atmospheric lensing

everyday, almost from anywhere on Earth. Because atmospheric lensing preserves surface brightness, just as in the case of gravitational lensing, the amplification of the mirage luminosity is simply equal to the ratio (i.e. magnification) of the solid angle of the observed image to that of the source image. Therefore, in addition to affecting significantly our view (image deformation, enlargement, multiplication, etc.) of distant resolved Earth-sources, atmospheric lensing is also often responsible for the light amplification of distant unresolved objects located along straight and long roads or across flat countrysides. As we shall see hereafter, there is quite some similarity between atmospheric and gravitational lensing. Let us first review shortly the history of gravitational lensing.

3. HISTORICAL BACKGROUND

Considering that light may be composed of elementary packets, Newton suggested as early as 1704 that the gravitational field of a massive object may bend light rays. However, because the wave description of light prevailed during the whole XVIIIth and XIXth centuries, the conjecture of Newton was not taken seriously. During the elaboration of his theory of General Relativity, Einstein predicted that a massive object does curve the spacetime in its vicinity and that any particle, massive or not (cf. the photons), will move along the geodesics of this curved spacetime. He predicted in 1916 that the apparent position of a star located near the solar limb should be displaced by 1.75", exactly twice the value that is derived from the classical Newtonian theory.

By using photographs of a stellar field taken during the solar eclipse in May 1919, Eddington and his collaborators (1920) were able to confirm the deflection angle predicted by Einstein. This was not only a triumph for General Relativity but also a marvelous confirmation of the concept that light rays may undergo deflections in gravitational fields.

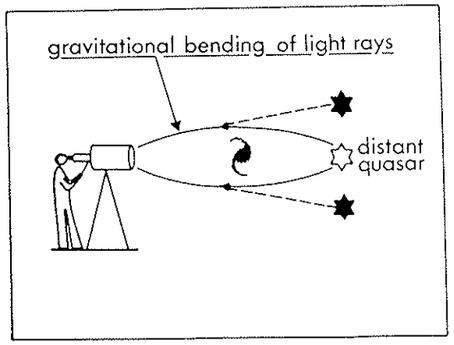

Figure 2: Gravitational lensing

Zwicky (1937a, b) was the first to realize the very high probability of identifying a gravitational lens mirage, i.e. made of several distinct images, among extragalactic objects (see Fig. 2). He even proposed to use galaxies as natural cosmic telescopes to observe otherwise too faint and distant background objects. He also emphasized the possibility of weighing the mass of distant galaxies by simply applying gravitational lens optometry.

After an inter-regnum of nearly 30 years, the interest for gravitational lenses was revived by Klimov (1963; galaxy-galaxy lensing), Liebes (1964; star-star lensing) and Zel'dovich (1964) and Refsdal (1964a, b, 1966a, b; cosmological applications of gravitational lensing). On a low level of activity, theoretical work continued through the seventies. Refsdal (1965, 1970) and Press and Gunn (1973) discussed problems on lens statistics, Bourassa et al. (1973) considered extended non-symmetric lenses and Dyer and Roeder (1972) derived a distance-redshift relation for the case of inhomogeneous universes. In spite of clear theoretical predictions, the interest from observers was rather low and no systematic search for lenses was initiated. However, fortytwo years after Zwicky's prediction, the dream of several astronomers finally became reality: Walsh, Carswell and Weymann discovered serendipitously in 1979 the first example of a distant quasar (0957+561) multiply imaged by a foreground massive galaxy. Following this pioneering detection, the levels of observational as well as theoretical activities increased dramatically, and today gravitational lensing constitutes a new important branch of astronomy.

4. PHYSICAL BASIS OF GRAVITATIONAL LENSES

4.1. General remarks

The physical basis of gravitational lensing essentially consists in the deflection of light, and electromagnetic waves in general, in gravitational fields as predicted by Einstein's theory of General Relativity.

In the regime of small deflection angles, which is of practical interest to us here, the so-called Einstein deflection of a light ray passing near a compact mass at a distance ξ is:

$$\hat{\alpha} = (4GM/c^2\xi) = 2R_{sc}/\xi \ll 1, \tag{1}$$

where G and c stand for the constant of gravitation and the velocity of light, respectively, and where R_{sc} represents the Schwarzschild radius of the mass M (see Fig. 3). The best measurements of the Einstein deflection have been made by means of radio interferometric observations of quasars close to the Sun, and confirm Einstein's value to nearly one tenth of a percent. In Newtonian terms, the Einstein deflection also follows if one assumes a refractive index n which depends on the Newtonian gravitational potential U via the relation $n = 1 - 2U/c^2$.

The great interest in gravitational lensing comes from the fact that this phenomenon can be used as a very powerful astrophysical tool. Indeed, it may help us in determining: (i) the size of the Universe (H_o) and possibly the values of other cosmological parameters (cf. q_o and Λ), (ii) the mass M and mass distribution of the lens, (iii) the nature and distribution of luminous and dark matter in the Universe, (iv) the size and structure of quasars, (v) the size of intergalactic gas clouds and (vi) the detection of random motions in the Universe, such as deviations from the Hubble flow. But before describing some of these potential applications, we shall introduce some basic concepts relevant to gravitational lensing.

Since the Einstein deflection is independent of wavelength, gravitational lenses are *achromatic*. Also, there is usually only one mass concentration which acts as a lens and which has a small extent relative to the cosmological distances involved: therefore the *thin lens approximation* is usually justified and the deflection can be considered as taking place at the location where the ray crosses the lens plane. Furthermore, *geometrical optics* can be used since physical optical effects are negligible in realistic situations.

Let now the true position of the source S on the sky be defined by the angle $\vec{\theta_S}$ and the image(s) position by $\vec{\theta_i}$ ($i = 1, 2, \ldots$). The *lens equation* which connects $\vec{\theta_S}$ and $\vec{\theta_i}$ is then simply given by

$$\vec{\theta_S} = \vec{\theta_i} - (D_{ds}/D_s)\vec{\hat{\alpha}}(\vec{\xi}) = \vec{\theta_i} - \vec{\alpha}(\vec{\xi}), \tag{2}$$

where D_{ds} and D_s represent respectively the "deflector- source" and "observer-source" angular size distances and where $\vec{\alpha}$ is the displacement angle, $\vec{\alpha} = (D_{ds}/D_s)\ \vec{\hat{\alpha}}$ (see Figs. 3 and 4). We note that a given source position may sometimes correspond to

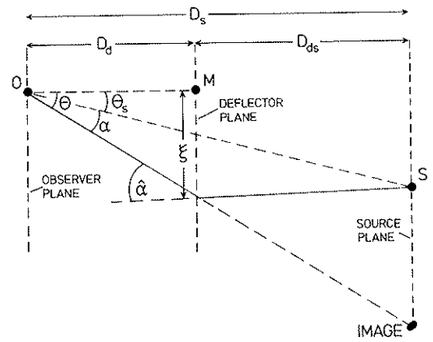

Figure 3: Deflection of a light ray due to a point mass lens

several distinct image positions whereas a given image position always corresponds to a specific source position. For the case of an extended lens and within the thin lens approximation, it is easy to calculate the effective deflection angle by just summing up the individual deflections due to all the mass elements (points) constituting the lens.

A typical lens situation is shown in Fig. 4, where source and image positions (one image in this case) are seen projected on the sky. We see again that the image position is shifted by $\vec{\alpha}$ relative to the source position; note however that $\vec{\alpha}$ is usually not constant over the source and this results in possible image deformations of extended sources.

Since gravitational lensing preserves the surface brightness of a source, the ratio (i.e. magnification) between the solid angle covered by the lensed image and that of the unlensed source immediately gives the amplification μ due to lensing. More formally, this is given by the inverse jacobian of the transformation matrix between the source and the image planes: $\mu = \mid \det(\partial\vec{\theta}_S/\partial\vec{\theta}) \mid^{-1}$.

If there are several images of a given source, the total magnification (amplification) is of course given by the sum of all individual image magnifications (amplifications). We suggest hereafter to use the term 'magnification' whenever the lensed images (cf. luminous arcs, radio rings, etc.) are resolved by the observer and the term 'amplification', otherwise (cf. when referring to micro-lensing effects).

4.2. The point mass lens

4.2.1. The model

Let us now describe the classical gravitational lens consisting of a single point mass (cf. a black hole or a very compact object). If the alignment of the source, the lens and the observer is perfect, all rays passing near the lens at a certain distance ξ_o will

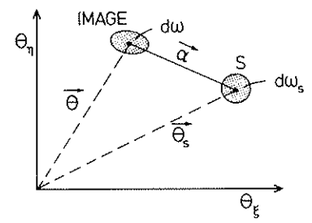

Figure 4: Image of a lensed source S as seen projected on the sky

Table 1: Angular (α_o) and linear (ξ_o) radii of the Einstein ring for different values of M and D_d , and $D_s = 2D_d$

M	D_d	α_o	$\xi_o = \alpha_o D_d$
1 $M_\odot$	10 kpc	7 10^{-4}"	10 AU
1 $M_\odot$	10^3 Mpc	2 10^{-6}"	10^{-2} pc
10^{12} $M_\odot$	10^3 Mpc	2"	10 kpc
10^{14} $M_\odot$	10^3 Mpc	20"	10^2 kpc

be bent towards the observer who will therefore see a very bright ring, the so-called *Einstein ring* (which should have been more properly named the Chwolson (1924) ring, cf. Fig. 5a). From Eqs. (1) and (2), it is easy to show that the angular radius of the Einstein ring is given by

$$\alpha_o = \frac{2}{c}\sqrt{\frac{GM D_{ds}}{D_d D_s}}. \qquad (3)$$

The value of α_o is very important because it can be used to estimate the angular separation between multiple lensed images in more general cases. Observed image separations ($\simeq 2\alpha_o$) can therefore lead to the value of M/D_d, or the value of M times the Hubble constant if the redshifts z_d and z_s are known. We see from Table 1 that for a source and a lens located at cosmological distances ($z_d \simeq 0.5$ and $z_s \simeq 1$), α_o can vary from micro-arcsec to some tens of arcsec, depending on the mass of the deflector.

For a slight deviation from perfect alignment, but retaining the lens symmetry, the Einstein ring breaks up in two bright images (cf. Fig. 5b). If the misalignment is further increased, one image approaches its normal luminosity whereas the second image, which is now seen very close to the lens, becomes fainter and fainter.

4.2.2. Optical depth for lensing

For the case of randomly distributed compact lenses, let us now estimate the frequency of gravitational lensing from observations of distant compact sources, i.e. objects and lenses whose angular size is definitely smaller than α_o.

Since the total magnification μ_T of a compact source lensed by a point mass lens exceeds 1.34 whenever the true source position lies inside the imaginary Einstein ring (i.e. for $\theta_S < \alpha_o$), the probability P to have significant lensing (by convention, $\mu_T >$ 1.34) for a randomly distributed compact source at a distance D_s is simply given by:

$$P = \frac{\pi\alpha_o^2}{4\pi} = \frac{D_{ds}GM}{D_s c^2 D_d} = -\frac{D_{ds}U}{D_s c^2}, \tag{4}$$

where $U(< 0)$ represents the Newtonian gravitational potential of the lens (at the observer). We see that the probability P is linear in U so that Eq. (4) is also valid for several deflectors acting independently of each other, irrespective of their individual masses. Considering a constant density of deflectors in a static universe, we may take an appropriate average of D_{ds} and derive the expression for the total probability P(or optical depth τ for lensing)

$$P = \tau = -\langle\frac{D_{ds}}{D_s}\rangle\frac{U_L}{c^2} = -\frac{U_L}{3c^2}, \tag{5}$$

where U_L is the gravitational potential at the observer due to all possible lenses at distances $D_d < D_s$. From this simple result, it is clear that stars in our Galaxy have an extremely small optical depth for lensing ($\mid U_L/c^2 \mid \simeq 10^{-6}$). The situation looks much more promising for distant sources. Following Refsdal (1965, 1970) and Press and Gunn (1973), it can be shown that

$$\tau = \frac{1}{4}\Omega_L\, z_s^2 \ , \text{ for } z_s \leq 1, \tag{6}$$

where z_s is the redshift of the source and Ω_L the cosmological density parameter of compact lenses. For $z_s > 1, \tau$ still increases with z_s but not as fast as indicated in Eq. (6). We see that values of τ near unity may be reached for $z_s \geq 1$ and that very distant cosmic sources constitute the best candidates for being lensed. Since the value of τ may be derived from the observed frequency of multiply imaged compact sources (quasars), we may use Eq. (6) to infer Ω_L and since $\Omega_L \leq \Omega_o$, a lower limit for the cosmological density parameter Ω_o results (see Section 6.3.1.).

4.3. Uniform disk lens

A transparent circular disk of matter, seen face on and having a radius r and

a uniform surface mass density Σ, is characterized by an effective deflecting mass $\pi\Sigma\xi^2, \xi(< r)$ representing the impact parameter for a chosen light ray. The latter will thus be deflected by the angle $\hat{\alpha} = 4\pi G\Sigma c^{-2}\xi$; the disk is actually acting as a normal converging lens with a focal length

$$f = c^2/(4\pi G\Sigma). \tag{7}$$

It is now easy to see that, by exact alignment, light from a distant point source focuses in the observer plane when

$$\Sigma = \Sigma_{\text{crit}} = c^2 D_s/(4\pi G D_d D_{ds}), \tag{8}$$

Σ_{crit} being the so-called critical surface mass density. It is interesting to note that $\Sigma_{\text{crit}} \simeq 1$ g cm^{-2} for typical cosmological distances, a value which roughly corresponds to the surface mass density in the central parts of massive galaxies, and that the average surface mass density inside an Einstein ring is Σ_{crit}. For extended deflectors, one must usually have $\Sigma \geq \Sigma_{\text{crit}}$ in at least some part of the deflector in order to create multiple images.

4.4. More complex lens models

Symmetric lenses are of course seldom realized in nature; usually the main lens itself is asymmetric or some asymmetric disturbances may also be induced by the presence of neighbouring masses. We may simulate in our optical experiment the effects of a typical non symmetric gravitational lens by just tilting the plexiglass lens. This has been done for the examples shown in Figs. 5c-g and results typically in image configurations which have been observed for the cases of two images (e), four images (c), and the optical luminous arcs (f) and Einstein radio rings of extended sources (g).

In an important paper, Burke (1981) has demonstrated that a non singular, transparent lens always produces an odd number of images for a given point source (except when located on the caustics). This is in apparent contradiction with the preferred even number of images observed in our lens experiment and in nature. If, however, our plexiglas lens would have been constructed non-singular in the centre, we would have seen an additional image formed in the central part of the lens. For the known lenses with an even number of observed images, it may well be that a black hole resides in the centre of the lens. The presence of a compact core could also account for the "missing" image since then the very faint image expected to be seen close to, or through the core, would be well below the detection limits that are presently achievable.

4.5. Time scales of gravitational lensing effects

Since for the case of asymmetric lenses the size of the diamond shaped caustic is usually comparable to the radius ξ_o of the Einstein ring associated with a compact object of similar mass, the typical lifetime t_o of a gravitational lens system should be

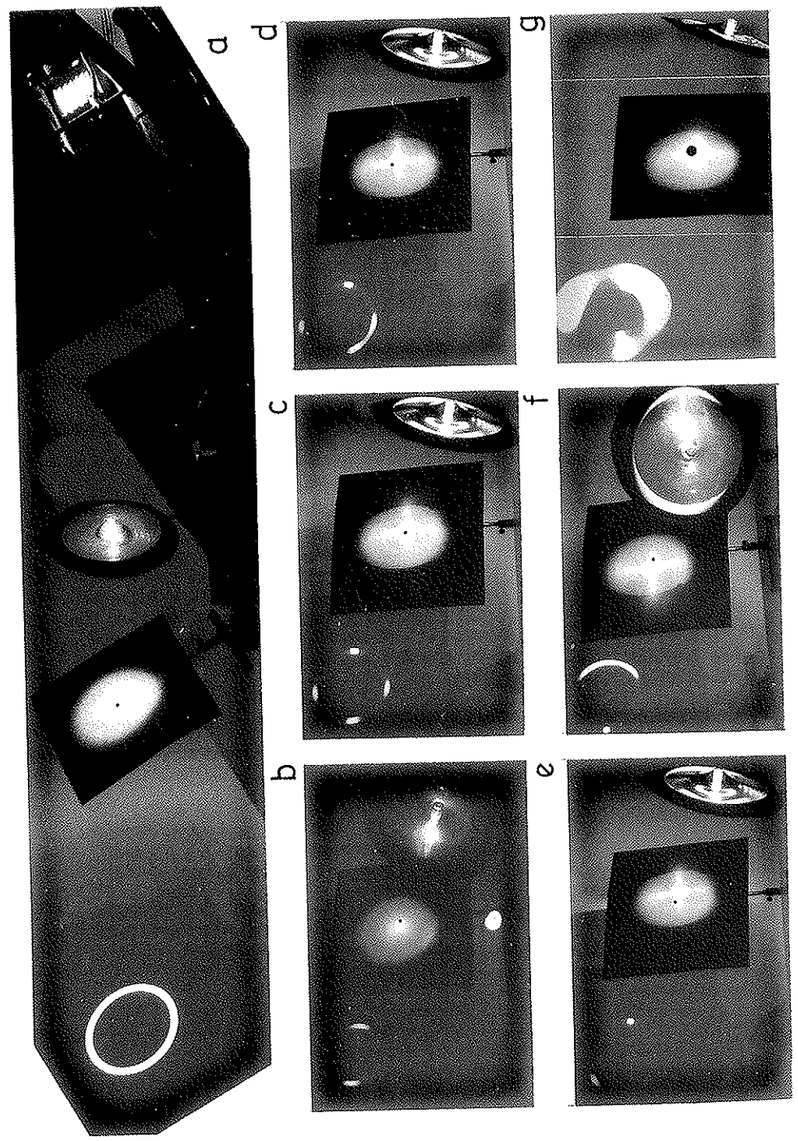

OPTICAL GRAVITATIONAL LENS EXPERIMENT (see Fig. 5)

The seven pictures to the left illustrate our optical gravitational lens experiment:
Fig. 5a shows the setup for the lens experiment. The compact light source is located on the right side (not clearly seen), then comes a plexiglass lens which deflects the light rays very nearly as a black hole with one third of the Earth mass ($R_{sc} \simeq 0.3$ cm). Behind the lens, we find a black screen with a small hole at the center (pinhole lens). Further behind, there is a large screen on which is projected the lensed image(s) of the source (the Einstein ring, in this case) as would be seen if our eye were located at the position of the pinhole. In the example illustrated here, the pinhole is set very precisely on the optical axis of the gravitational lens so that the source, the lens and the pinhole (observer) are perfectly aligned. Note that the bright regions seen on the lens are caused by scattered light.
Fig. 5b illustrates what happens when the pinhole (observer) is moved slightly away from the symmetry axis: the Einstein ring breaks up in two images.
Fig. 5c then shows the resulting four lensed images when the optical lens is somewhat tilted around the vertical axis. In this case, the bright line along the optical axis which existed in the symmetric configuration (cf. Fig. 5a) has changed into a two dimensional caustic surface, a section of which is seen as a diamond shaped caustic (made of four folds and four cusps) in the pinhole plane. The four lensed images observed here arise when the pinhole (observer) lies inside the diamond formed by the caustic.
Fig. 5d shows the merging of two images into one bright image when the pinhole approaches one of the fold caustics. Due to the large amplification (magnification) and short time scale during the crossing of such a caustic, there results a High Amplification Event (HAE).
Fig. 5e: Here, the pinhole (observer) is located just outside the diamond. The two merging images have now disappeared.
Fig. 5f shows the image configuration when the pinhole is located very close to one of the cusps. One observes in this case a very nice luminous arc and a much fainter counterimage.
Fig. 5g illustrates the lensed image(s) when the pinhole size is increased by a factor $\simeq 4$, equivalent to a significant increase in the source size. In this example, an almost complete ring is observed, although the source, lens and observer are not perfectly aligned and the lens is still being tilted.

the time it would take for an observer (the pinhole) to cross the radius $x_o = \xi_o D_s/D_{ds}$ of the Einstein ring projected onto the observer's plane. The relative motion between the observer and the caustic may be thought of as arising from the relative velocities between the observer, the lens and the source. If V represents the effective transverse velocity of the observer, then the typical lifetime t_o of a gravitational lens system is given by

$$t_o \simeq x_o/V. \tag{9}$$

Referring to Table 1 and assuming $V \simeq 600$ km s^{-1}, we see that for typical cosmological distances and for the case of a massive galaxy lens, we obtain $t_o \simeq 2\ 10^7$ yr, whereas for a one solar mass star acting as a lens, we get $t_o \simeq 20$ yr. If the star is in our Galaxy ($D_d \simeq 10$ kpc), we get a typical lifetime of just a few months ($V \simeq 200$ km s^{-1}). The time scale for merging and disappearance of lensed images, as shown in our experiment, can be much shorter than the time scales given above; this will be discussed later.

5. OBSERVATIONS OF GRAVITATIONALLY LENSED OBJECTS

As it will become apparent in this section, the previous optical gravitational lens experiment turns out to be very useful in order to understand the various types of image configurations that have been observed for the different known lens systems in the sky.

Before presenting such observations, we shall first describe very briefly some of the (optical and radio) surveys which are being carried out at several major ground-based observatories in order to search for gravitational lensing effects.

Among the optical lens surveys, we should like to mention the search for multiply imaged quasars within a sample of highly luminous quasars (HLQs), i.e. quasars whose absolute magnitude in B is typically brighter than -28 (Surdej et al. 1988). An ESO-key programme is presently dedicated to such a survey with parallel and also independent observations obtained at other major observatories (CFH, Las Campanas, CTIO, Palomar, NOT at La Palma, NRAO).

The observations consist first in obtaining direct multi-color CCD frames of quasars under the best possible seeing conditions. When multiple images of a distant quasar turn out to show similar colors, they are then observed spectroscopically. If the spectra appear to be identical, one performs a deep imaging of the system in red light to try detecting directly the lens. Among the ten or so known lensed quasar candidates, more than two thirds correspond to HLQs. The reason is in fact simple: it is due to an observational bias (the so-called 'magnification' bias). Indeed, the probability of including a quasar that has been magnified by gravitational lensing effects is greater in a flux limited sample than in a volume limited one, and since only flux limited samples are being used, this bias naturally accounts for the observations.

The signature of gravitational lensing effects is also searched for in larger samples of normal quasars, which are of course less affected by the magnification bias. Such surveys are actually being performed all over the world.

Also very interesting are the systematic optical surveys for the detection of giant luminous arcs near rich foreground galaxy clusters that have recently been initiated by several teams of european and north and south american astronomers (Toulouse, Meudon, AT&T Bell Laboratories, Princeton, Barcelona). The detection of such arcs, characterized by a very low surface brightness, essentially relies on the good quality of the site (seeing, darkness of the night, etc.) and on the sensitivity of the instrumentation used (large telescopes, CCDs with low read-out-noise and high quantum efficiency, long exposure times, etc.).

Let us now describe two radio surveys for lensing effects. We wish specially to mention the VLA snapshot survey, at 5 GHz. It consists in a search for lensed objects among some 4200 high galactic latitude radio sources chosen from the MIT-Greenbank catalogue. With an angular resolution of typically 0.3", this survey should produce a statistically well defined sample of more than ten lens systems. Several discoveries of such gravitational lenses have already been reported (Hewitt et al. 1987). The other survey consists of the flux limited radio sample of 3C and 4C distant sources which are being imaged optically at high angular resolution both at ESO and at the CFHT. Because these samples are also subject to a (double) magnification bias (Borgeest et al. 1991), it is not surprising that several good gravitational lens candidates have been reported in the past (see Hammer and Le Fèvre 1990).

A photometric monitoring survey for micro-lensing effects is presently conducted by the Hamburg lens group in Calar Alto (Spain). It consists in a program of direct CCD imagery of a selected sample of 100 quasars (known GLs, HLQs, quasars near galaxies, narrow absorption line QSOs, Blazars, etc.). Photometric monitorings of known GLs are also being made at ESO and with the NOT at La Palma.

Last but not least, in order to prove the possible existence of dark massive compact objects in the halo of our Galaxy, Paczyński (1986) has suggested to search for induced micro-lensing effects by the former objects on the light emitted from background stars. Two major observational projects aiming at the detection of micro-lensing effects of Magellanic Cloud stars by foreground compact halo objects have been recently initiated by a French group and an American-Australian team of astronomers at ESO and Mt. Stromlo, respectively.

5.1. Individual lensed objects

By now, there are about 10 proposed cases of multiply imaged quasars, 5 radio rings and more than 10 examples of giant luminous arcs and arclets. Because of space limitation, we shall only describe some of these.

5.1.1. Multiply imaged quasars

We shall first have a look at some examples of multiply imaged quasars belonging

Table 2: Observational information relevant to Figure 6a-j

Fig.	Source name	Image(s)	Waveband
6a	0957+561	A-B + Lens	Optical R + Radio
6b	0142-100	A-B	Optical R
6c	0142-100	Lens	Optical R
6d	1115+080	A-D	Optical R
6e	2237+0305	A-D + Lens	Optical R
6f	1413+117	A-D	Optical R
6g	MG1131+0456	A-B + Ring	Radio
6h	MG1654+1346	Ring	Radio
6i	Abell 370	Arc	Optical B
6j	Cl2244-02	Arc	Optical B

to the two major classes of image configurations (i.e. 2 or 4 images). In the two image configuration (cf. Fig. 5e), the lensing galaxy is usually located between the two images. In the four image configuration (cf. Fig. 5c), the QSO images lie roughly on a circle; the lensing galaxy being located near its center.

0957+561: The first reported example of a multiply imaged quasar (0957+561) consists of two components (A and B) at a redshift $z = 1.41$, separated by 6.1", accompanied by an extended radio source (see Fig. 6a and Table 2). The lensing galaxy at $z = 0.36$ is found to lie very near ($\simeq$ 1") the southern component. This galaxy is a member of a rich cluster whose mass also contributes to the lensing. 0957+561 has turned out to be very important from the point of view of cosmological applications (namely the possible determination of the Hubble parameter H_o by means of the measurement of the time delay Δt, see Section 6.1.).

0142-100: This is the first gravitational lens system that has been discovered at ESO in a systematic survey among HLQs (Surdej et al. 1987). The two QSO images ($z = 2.72$) are separated by 2.2" (see Fig. 6b) and their spectra turn out to be identical. After subtracting from the observed QSO images a double point spread function (PSF), the lens of this system is seen and it appears to be made of a single isolated galaxy at a redshift $z = 0.49$ (cf. Fig. 6c). The mass of this deflector (within an angular radius of 1.1") has been estimated to $\simeq 2.4\ 10^{11}\ h_{50}^{-1} M_\odot (h_{50} = H_o/50$ km s^{-1} Mpc^{-1}). Because no trace of a galaxy cluster has been detected around the lensing galaxy, this system constitutes a clean and good candidate to attempt an independent determination of H_o. The expected time delay is of the order of 7 weeks. A photometric monitoring of this system is under way at ESO and with the NOT. However, because of scheduling constraints, uncertain weather and seeing conditions, it is very difficult to get sufficiently well sampled lightcurves. We should like to stress here that the

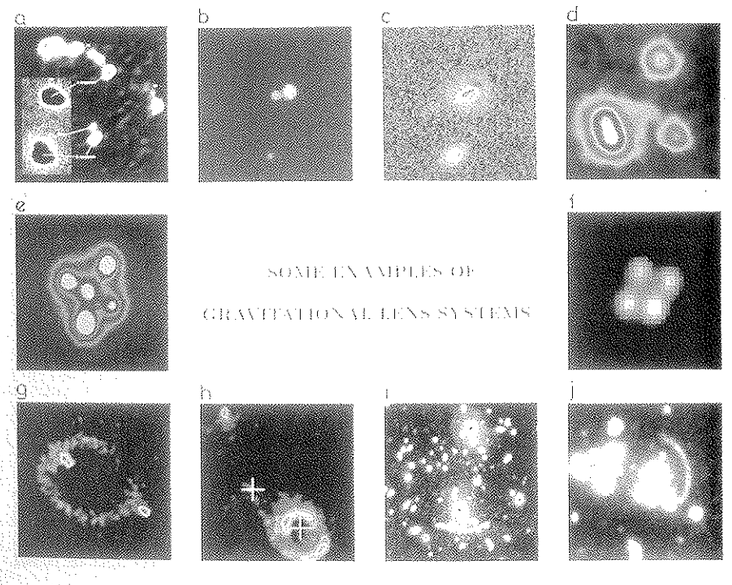

Figure 6: Some examples of known gravitational lens systems (a-j)

possible use of a 2-3 m class optical telescope, fully dedicated to the monitoring of known gravitational lens systems, would most probably bring just after a few years of continuous observations major contributions in the fields of cosmology and physics of quasars.

1115+080: By means of the pupil segmentation technique used with the CFH telescope (Lelièvre et al. 1988), high angular resolution observations of PG1115+080 ($z = 1.72$) have been obtained in the past (see Fig. 6d). This so called "Triple Quasar", discovered serendipitously by Weymann and his collaborators in 1980, does actually consist of 4 images: component (A) is a nearly merged double image whose separation is just 0.5" (cf. Fig. 5d). The time delays between the different pairs of the 4 images range from some days to several months. A lensing galaxy ($z = 0.305$) has been detected between the A and B images.

2237+0305 (the Einstein Cross): This is another example of a multiply imaged quasar identified serendipitously by Huchra and his collaborators in 1985, during a survey of galaxy redshifts. First of all, superb high angular resolution imaging (cf. Fig. 6e) and spectroscopy have convincingly demonstrated that the Einstein cross consists of four lensed images ($z = 1.69$, with angular separations between 1.4" and 1.8") plus a central galaxy nucleus ($z = 0.04$). The mass of the deflector inside the 4 lensed images is about $2\ 10^{10} h_{50}^{-1}\ M_\odot$. This system is unique for displaying micro-lensing effects (Kayser and Refsdal 1989). Indeed, because the expected time delays are so short (at most a few days), intrinsic variability should show up almost simultaneously in the four images so that any brightness variation affecting just some of the four single images may be attributed to micro-lensing. Also, due to the large distance ratio between the source and the lens, micro-lensing should lead to more frequent and rapid high amplification events (HAEs) and the expected number of HAEs should be large (about 0.3 events per year and per image). It was therefore not a surprise when Irwin et al. (1989) announced a significant brightening of only component A. CCD frames taken at La Silla in the framework of the ESO key-programme and with the NOT indicate that at least three of the four images are affected by micro-lensing effects. In particular, the visual brightness ratio A/B has recently been observed to vary from about 1.3 to 0.8 in less than one year. Theoretical analysis of these data favors relatively small masses for the micro-lenses; it is however not necessary at the moment to invoke masses below 0.1 $M_\odot$ (Wambsganss et al. 1990). With more data, one should also be able to set interesting constraints on the size and the structure of the QSO (cf. Section 6.2.).

1413+117 (the Clover Leaf): This is the second example of a multiply imaged QSO ($z = 2.55$) that has been identified at ESO, within a systematic search for lenses among HLQs (Magain et al. 1988, cf. Fig. 6f). High angular resolution (FWHM $\simeq$ 0.6") integral field spectroscopy of this system obtained with the bidimensional spectrograph SILFID at the CFHT has enabled one to resolve the spectra of the four individual images. The spectra, which show characteristic broad absorption line profiles, turn out to be very similar, except for narrow absorption line systems (probably related to the lens(es)) seen in images A and B and also for small but significant differences in the spectrum of image D which are probably due to micro-lensing effects (Angonin et al. 1990).

5.1.2. Radio rings

This new class of lensing phenomena, first discovered with the VLA, occurs when some part of the extended radio source covers most of the diamond shaped caustic associated with the lensing object (cf. Fig. 5g). The resulting lensed image consists then of a slightly elliptical ring of radio emission.

MG1131+0456: Maps of the radio source MG1131+0456 in Leo has revealed such an elliptical ring of emission with two compact sources lying on opposite sides of the ring (angular separation $\simeq 2\alpha_o \simeq$ 2.1", see Fig. 6g). It was found by J. Hewitt and her collaborators in 1988. A very sophisticated modeling of this lensed radio source has been reported by Kochanek et al. (1989). Their numerical inversion of the observed mirage leads to a normal galaxy-like elliptical potential for the lens and an ordinary double-lobed structure for the background radio source. In this model, the two compact images correspond to the lensing of the central core of the source while the ring is associated with a radio jet which covers most of the diamond shaped caustic in the source plane.

MG1654+1346: A second ring was found in Hercules by Langston et al. in 1989. A deep red optical CCD frame of MG1654+1346 shows only an elliptical galaxy ($z = 0.25$) and a quasar ($z = 1.74$) located 2" away (see the two crosses in Fig. 6h). However, VLA radio maps at 3.6 cm reveal that the foreground galaxy lenses one of the quasar's radio lobes into a ring having an angular diameter of 2.1" (cf. the contour levels in Fig. 6h). From the angular size of the radio ring, it is easy to show (cf. Eq. (3)) that the mass of the deflecting galaxy (projected inside the ring) is about $3\ 10^{11} h_{50}^{-1}\ M_\odot$.

5.1.3. Giant luminous arcs and arclets

We shall now describe a last class of lensing phenomena consisting of the fascinating optical giant luminous arcs and arclets.

The first giant luminous arcs (angular extent $\simeq$ 20", angular width $\leq$ 0.5") were discovered serendipitously in 1986 by Soucail and Fort and by Lynds and Petrosian plus their collaborators, in the centres of rich clusters of galaxies (mass $\simeq 10^{14}\ M_\odot$). As suggested by Paczyński (1987), the measurement of several arc redshifts has confirmed that they result from the gravitational lens distortions of distant background galaxies by rich foreground clusters acting as lenses (cf. Fig 5.f). Up to now, about 10 giant arcs, whose surface brightness is only about one tenth of the sky brightness, have been identified in rich clusters; half of them have a measured redshift which, in all cases, is larger than that of the cluster.

Abell 370: The A370 arc (see Fig. 6i) has been found to be the gravitational image of a background source ($z = 0.72$). This source is most probably a nearly edge-on spiral galaxy, lensed by a rich foreground cluster ($z = 0.37$).

Cl2244-02: The core of the cluster Cl2244-02 seems to be dominated by galaxies that belong to two clumps. The detected arc (full angular extent $\simeq 110°$, see Fig. 6j) consists of the gravitationally lensed image(s) of a background source, which is probably a star-forming galaxy at a redshift $z = 2.238$. This is one of the most distant regular galaxies that has been observed and it clearly shows how gravitational lenses may be used as cosmic telescopes to detect very faint and distant galaxies.

6. COSMOLOGICAL AND ASTROPHYSICAL APPLICATIONS

6.1. Determination of the Hubble constant H_o and the mass of the lens

We shall address now one of the most interesting cosmological applications of gravitational lensing: the determination of the Hubble constant H_o via the measurement of the time delay Δt between the observed lightcurves of multiply imaged QSOs. We discuss hereafter the wavefront method for the case of a symmetric lens as it was first proposed, although in a slightly less obvious form, by Refsdal (1964a, b); a somewhat clearer presentation has been given by Chang and Refsdal (1976). An alternative way of calculating Δt was suggested by Cooke and Kantowski (1975), they showed that the time delay could be split into two parts, a geometrical time delay and a potential time delay.

With the wavefront method, a simple expression for Δt can be obtained for the case of an axially symmetric lens by considering the wavefronts from a distant QSO as drawn in Fig. 7. Since the wavefronts are crossing each other at the symmetry point E, they must represent the same light propagation time and for an observer O located at a distance x from the symmetry axis, the time delay must be equal to the distance between the wavefronts at the observer divided by the velocity of light. Noting that θ_{AB} is very small, we thus obtain from simple triangle geometry

$$\Delta t \simeq \theta_{AB} x c^{-1}. \tag{10}$$

Furthermore, we easily find that

$$\theta_S = x D_{ds}/(D_d D_s). \tag{11}$$

Assuming a deflection law of the type

$$\hat{\alpha} \propto \xi^{(\epsilon-1)} \tag{12}$$

between the impact parameters ξ_A and ξ_B , we find a simple relation between θ_A, θ_B and θ_S

$$\theta_S = (\theta_A - \theta_B)(2 - \epsilon)/2. \tag{13}$$

It is very simple to derive Eq. (13) for the case $\epsilon = 1$, and it is also accurate for $\epsilon = 0$ and $\epsilon \to 2$. For intermediate values of ϵ, this equation is not exact but it is nevertheless

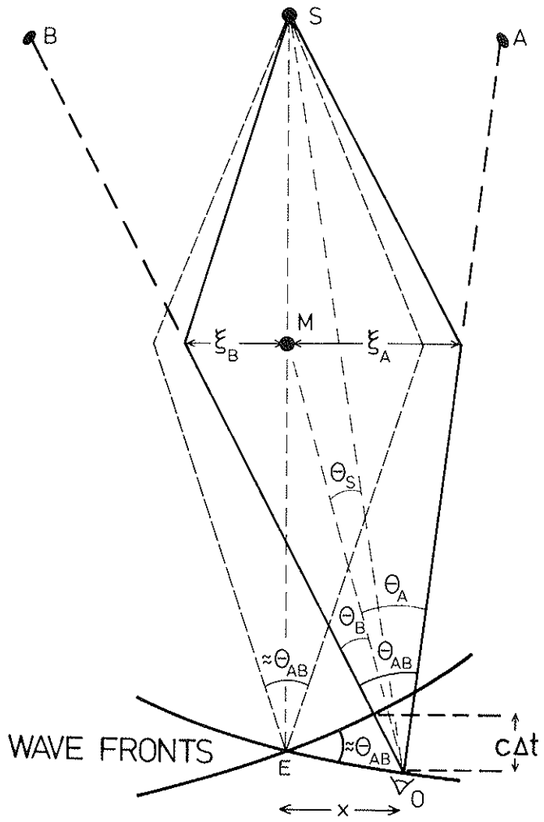

Figure 7: The wavefront method for the determination of the time delay

accurate enough for the purpose of our discussion. On the basis of the above equations and making use of the Hubble relation for the deflector and the source

$$D_d = cz_d H_o^{-1}, D_s = cz_s H_o^{-1}, \tag{14}$$

we can easily derive an expression for H_o in terms of observable quantities

$$H_o = \frac{z_d z_s \theta_{AB}(\theta_A - \theta_B)(2-\epsilon)}{(z_s - z_d)2\Delta t}. \tag{15}$$

For the case of the double quasar 0957+561 A and B, we know the observed positions $\theta_A = 5.1$" and $\theta_B = 1.04$", from which we derive

$$H_o = 140(2-\epsilon)(\frac{1 \text{ year}}{\Delta t})km\ s^{-1}\ \text{Mpc}^{-1}. \tag{16}$$

Based upon a much more sophisticated model which takes into account all available observational data (image and lens positions, redshifts, time delay, luminosity ratios and radio data) and considering a King-type model for the deflecting galaxy, a point mass object in the centre and a linearized cluster, Falco et al. (1991) have derived the following expression for H_o

$$H_o = (90 \pm 10)(\frac{\sigma_v}{390km\ s^{-1}})^2(\frac{1 \text{ year}}{\Delta t})km\ s^{-1}\ \text{Mpc}^{-1}, \tag{17}$$

where σ_v represents the velocity dispersion of the deflecting galaxy. For $\sigma_v < 390$ km s^{-1}, the galaxy cannot do the whole lensing alone; the effects due to the cluster must be taken into account and this has of course direct consequences for the determination of H_o. Equations (15) and (16) could also have been generalized to include such a σ_v correction term by simply modeling the cluster as a uniform circular disk with a surface mass density $\Sigma = (1 - (\sigma_v/390)^2)\Sigma_{\text{crit}}$(cf. Section 4.3). We then see that for $\epsilon \simeq 1.36$, Eq. (16) leads to the same result as Eq. (17). This does not seem to be unreasonable in view of the large core radius that Falco and his collaborators have derived from their best fit model, in spite of the small compact mass in the centre which slightly reduces ϵ.

Which value of H_o do we now get from Eq. (17)? Rhee (1991) has recently measured the value $\sigma_v = 303 \pm 50$ km s^{-1} for the velocity dispersion of the lensing galaxy; this value should however be increased by a factor $\sqrt{1.5}$ in order to account for the lensing effects caused by its probable dark halo which has a larger velocity dispersion. In any case, a considerable part of the lensing must also be attributed to the cluster. The results from recent optical as well as radio monitoring campaigns of 0957+561 A and B seem to indicate a time delay of 1.45 ± 0.1 yr (Press et al. 1991), although a value near 1.14 yr cannot yet be totally excluded (Vanderriest et al. 1992). Inserting in Eq. (17) all these data and taking into account a small cosmological correction factor (about $\pm 10\%$), we finally end up with a value for H_o that is in good agreement with those derived using conventional methods,

$$H_o = (55 \pm 25)km\ s^{-1}\ \text{Mpc}^{-1}, \tag{18}$$

in a somewhat better agreement with the 'school' that favors a low value for H_o. Please note that since the observed separation ($\simeq 2\alpha_o$) between multiply lensed images scales as $\sqrt{MH_o}$ (see Section 4.2.1.) and making use of the simple relation between the time delay Δt and H_o(i.e. $\Delta t \propto H_o^{-1}$, cf. Eq. (15)), one may determine the mass M of the galaxy deflector, located within an angular radius $(\theta_A + \theta_B)/2$, from the direct measurement of the time delay Δt, irrespective of the Hubble constant. A more detailed examination shows that this mass determination is also independent of the presence of the cluster and of the cosmological model (Borgeest 1986). For the case of 0957+561, Borgeest has derived the lens mass $M = (1.1 \pm 0.2)10^{12}(\Delta t/1.45\ \text{yr})M_\odot$. We note however that the determination of H_o may be strongly influenced by the cluster. Due to a degeneracy in the estimate of system parameters (Gorenstein et al. 1988), it is not possible to determine the cluster correction term only from observations of 0957+561 A and B. This is an important and general result, also valid when more than two images are observed. Independent information on the mass of the galaxy and/or the cluster is needed. This information is provided in Eq. (17) by means of the σ_v term. Let us however note that this correction term depends critically on our understanding of galaxy dynamics, unless detailed measurements of the velocity field become available for many different regions in the lensing galaxy.

6.2. Micro-lensing

6.2.1. Generalities

We come now to another interesting aspect of lensing phenomena, the so-called micro-lensing due to individual stars (Chang and Refsdal 1979), or other compact objects having a similar or even a lower mass, usually located in a galaxy which acts as a macro-gravitational lens. Since the angular sizes of quasars are smaller than, or comparable to, the Einstein ring of a star, this can lead to a splitting-up of each QSO macro-image into several micro-images, with typical angular separations of some micro-arcsec. Of course, these are not resolvable with techniques available today; however, the integrated luminosity observed for all those micro-images will vary with time due to the transverse motions of the stars. It is therefore an important and very interesting phenomenon. A simple way of visualizing the effects of micro-lensing is by the so-called ray plot diagram (Kayser et al. 1986), which consists in a mapping of a regular grid of points in the deflector plane onto the observer plane (source plane). One can easily show that, apart from a scaling factor, the ray plots in the observer plane are identical to those in the source plane. An example of such a diagram, constructed by a simpleminded ray shooting (inverse ray shooting), is shown in Fig. 8 where the randomly distributed stars, here all with the same mass M, correspond to an optical depth for micro-lensing $\tau = 0.4$. This means that the Einstein rings of the stars cover a fraction 0.4 of the sky and that the smoothed out surface mass density of the stars is 0.4 Σ_{crit}.

The density of points in a ray plot is directly proportional to the flux of the amplified macro-image under consideration if the source is point-like. For extended sources with a constant surface brightness, the flux is simply proportional to the number of points covered by the source. It is interesting to see that the same diamond shaped caustic structures appear in the ray plot as in the optical lens experiment. Now, however, the diamond shaped caustics are obviously distorted by the neighbouring stars. If we neglect the motions of the deflecting stars relative to one another, the corresponding ray plot will not change with time. However, due to the relative transverse motion between the source, the star field and the observer, the source will move across the ray plot, causing a variation of its brightness with time. It thus becomes clear that light variations caused by micro-lensing are greater and faster for small sources than for large ones, as clearly seen in Fig. 8. These lightcurves were constructed by moving sources with different sizes along the middle track indicated in the ray plot. The length unit in the ray plot diagram was chosen to be the radius of the Einstein ring, projected into the source plane, which for cosmological distances is typically $x'_o = (D_s/D_d)\xi_o = 0.01\sqrt{M/M_\odot}$ pc, corresponding to a time scale of

$$t_o = x'_o/V' \simeq 20yr\sqrt{M/M_\odot}(600km\ s^{-1}/V'), \tag{19}$$

where V' is the effective transverse velocity in the source plane; compare with Eq. (9).

Since micro-lensing variability occurs independently for the different macro-images, this effect may complicate the determination of the time delay from the observed photometric lightcurves. Also, when modeling macro-lensed images, one must consider with caution the observed luminosity ratios of compact sources. Note, however, that the observed positions of the macro-lensed images are little affected by micro-lensing.

Gravitational lenses are basically achromatic but since the amplification factor due to micro-lensing depends on the source size, indirect chromatic effects may result if the source size depends on wavelength. In particular, the continuum source and the (much larger) broad emission-line regions may be differently magnified, causing differences between the equivalent widths of emission-lines observed in the spectra of the macro-images. Even small differences in the emission-line profiles may occur.

The best candidates expected to show strong micro-lensing effects are those quasars already multiply imaged (macro-lensing). Indeed, since we know that there is so much mass located "between" the lensed images, we may reasonably expect a large optical depth for micro-lensing. Only if a very small fraction of the lensing mass is in the form of compact objects or if the mass distribution is strongly concentrated towards the centre of the macro-lens, should we expect a small optical depth for such systems. Photometric monitoring of multiply imaged quasars is therefore a very promising way to get information on dark matter in distant galaxies. We should learn soon from such studies whether dark matter is in large clumps, compact enough to produce micro-lensing effects, or in the form of much more uniformly distributed material.

6.2.2. High Magnification Events (HMEs)

Of special interest are the so-called high amplification events (HAEs) which occur

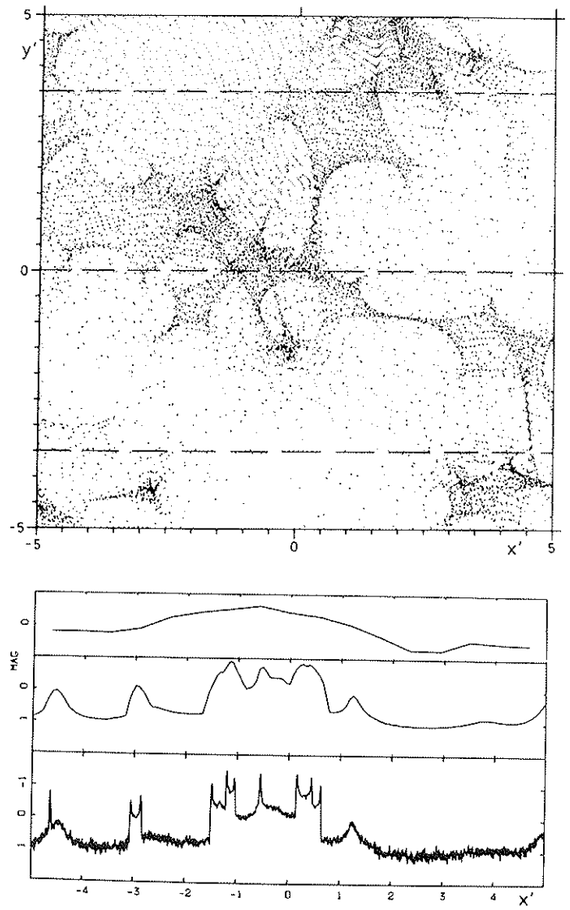

Figure 8: Ray plot diagram (above) for an optical depth $\tau = 0.4$ and corresponding lightcurves (below) for three different sources with radii $\simeq x'_o, 0.1x'_o$ and $0.01x'_o$, respectively. The simulated lightcurves correspond to motions of the source along the middle track drawn in the ray plot diagram. One unit along the x' and y' axes corresponds to x'_o, the radius of the Einstein ring projected onto the source plane. For typical cosmological distances, we expect that one unit in this diagram corresponds to $\simeq 20.\sqrt{M/M_\odot}yr$, see Eq. (19).

when the source (or observer) crosses a caustic. For compact sources, one gets typical asymmetric peaks in the lightcurve of the relevant macro-image (see Fig. 8). We saw in our optical lens experiment that the number of micro-images then changes by two. Thus an HAE resembles an eclipse phenomenon. It is then obvious that the time scale ∂t for the steep rise (or decline) of the lightcurve is given by

$$\partial t \simeq 2R_s/V'_N, \tag{20}$$

where V'_N is the component of V' along the normal to the caustic and R_s the radius of the source. We shall see hereafter how it is possible to infer independently the value of V'_N such that R_s can be determined. By analysing the lightcurve observed during an HAE, it becomes then even possible to retrieve the intrinsic one-dimensional brightness profile of the source following a method similar to that used for stellar eclipsing binaries (Grieger et al. 1988). However, in contrast to a normal eclipse, we must take into account the increasing amplification μ of the merging micro-images as the source approaches the caustic ($\mu \propto d^{-1/2}$, where d is the distance to the caustic; this is a generic property of caustics). The results of numerical simulations have shown that one-dimensional profiles can usually be retrieved for sources whose radius is typically less than one tenth of the projected Einstein radius, which corresponds to a few light days for solar mass stars and cosmological distances (Grieger et al. 1988).

6.2.3. The parallax effect

We have just seen that micro-lensing causes flux gradients in the observer plane, so that a brightness difference

$$\delta m = \mathrm{grad}(m)\delta\vec{r} \tag{21}$$

is observed by two observers located at a distance $\delta\vec{r}$ from each other. This effect is often referred to as the parallax effect (Grieger et al. 1986). Expected values of grad(m) are typically between $10^{-4}\ AU^{-1}$ and $10^{-3}\ AU^{-1}$, but during HAEs values up to $10^{-2}\ AU^{-1}$ may be reached (assuming that $R_s \simeq 10^{-3}$ pc and $M \simeq M_\odot$). For two observers (1 and 2) located some AU apart, it should then be possible to determine the time lag $\delta t_{1,2}$ between the photometric lightcurves recorded during an HAE and thereby get information on the velocity V_N (perpendicular component to the local caustic tangent) by which the caustic is sweeping through the solar system. Neglecting the "small" velocity of the observers relative to the Sun and the very small curvature of the caustic, we get

$$V_N = r_{1,2}\sin(\beta)/\delta t_{1,2} \leq r_{1,2}/\delta t_{1,2}, \tag{22}$$

where $r_{1,2}$ represents the projected distance between the observers into the observer plane (perpendicular to the line-of-sight) and β is the angle between the line connecting the two observers and the caustic. Since β is not known, we obtain an upper limit on V_N. In the presence of a third observer (3), a second time lag may be derived and it

then becomes possible to get a point value for V_N. Taking into account the redshifts of the source and of the lens and assuming a cosmological model, we can determine V'_N(in the source plane) and thereby R_s from Eq. (20). We note that such velocity determinations have a great value in themselves since they should also allow one to probe possible deviations from the Hubble flow. Assuming V'_N to be about 600 km s^{-1}, we note that this corresponds to approximately one AU in 3 days; one would therefore expect a time lag of about one month between a terrestrial observer and an observer located close to Saturn.

From the known micro-lensing variability ($\simeq$ 0.1 mag/month) reported for the A image in the Einstein Cross (2237+0305, see Section 5.1.1.), it is clear that simultaneous observations of this system with even a modest space observatory passing near Saturn should allow one to measure the time lag δt.

An interesting point in connection with the measurement of a time lag is that it would immmediately prove that we are dealing with micro-lensing variability and not with intrinsic variations since the latter ones would only produce extremely small time lags which can easily be corrected for. This is particularly important for sources with only one macro-image since then the distinction between the two types of variability is very difficult to establish by other means.

Considering baselines of the order of $100AU$ or even larger, we expect that most distant quasars should show small brightness differences. Observations of a large number of quasars would then provide very valuable information on the mass distribution in the Universe (masses between $\simeq 0.001M_\odot$ and $\simeq 100M_\odot$). One should note that the space observatories needed to achieve these goals could be mostly dedicated to other scientific projects and that the applications suggested here would just consist in by-products of great astrophysical importance.

6.3. Search for dark matter

Various types of lens observations can provide us with information on dark matter in the Universe. This is a field which is still in its infancy, but with a great promise for the future.

6.3.1. Search for compact lenses

As already discussed in Section 4.2.2., the frequency of multiply imaged sources (e.g. quasars) depends on the cosmological density parameter Ω_L of compact objects. Let us however note that a magnification bias may strongly influence the results derived from flux limited samples of quasars (cf. Section 5). Since the highest angular resolution achievable today is slightly below 10^{-3}"$(VLBI)$, masses down to $10^4M_\odot$ can in principle be searched for at cosmological distances; see Eq. (3). From presently known surveys of quasars, Surdej et al. (1992) conclude that $\Omega_L < 0.02$ in the mass range $10^{10.6}M_\odot - 10^{11.8}M_\odot$, with a 99.7% confidence level. From the VLA snapshot survey (resolution $\simeq$ 0.3"), lensing compact objects with masses down to $\simeq 10^{10}M_\odot$ may be searched for, and the conclusion is similar: the density of compact objects is

well below the critical density ($\Omega_L \ll 1$). VLBI observations seem to exclude $\Omega_L \geq 1$ for masses down to about $10^5 M_\odot$, but many more observations are needed in order to better constrain limits on Ω_L.

An original way of searching for compact objects in the Universe with a mass in the range $10^{-3} M_\odot - 100 M_\odot$ is based upon the detection of micro-lensing effects which produce characteristic light variations of distant compact sources (cf. quasars). Particularly promising are the multiply (macro-) imaged quasars whose lensing galaxy should have a large optical depth for micro-lensing. We expect that important information on the nature of dark matter in these galaxies will be derived (see also Section 6.2.1.). For single isolated quasars, it is however more difficult to distinguish micro-lensing variability from intrinsic light variations, and observations of a large number of quasars over many years are in any case necessary in order to set reasonable limits on Ω_L.

As mentioned in Section 6.2.3., the parallax effect with a large baseline ($\simeq 100 AU$) also offers very exciting possibilities to "detect" compact masses in the range given above.

6.3.2. Luminous arcs and arclets

As seen in Section 5.1.3., the angular radius of the luminous arcs observed near rich foreground clusters is typically 20" and the mass inside the corresponding Einstein ring must therefore be about $10^{14} M_\odot$. This gives already strong evidence for the presence of large amounts of dark matter in the clusters and/or in the lensing galaxy lying close to the center of the arc.

Since giant luminous arcs represent cases of strong lensing by clusters, we know that cases of weak lensing of background galaxies must occur much more frequently. The main effect of such a weak lensing consists in a slight distortion of the lensed galaxies. This is however difficult to measure because the intrinsic distortion may vary from source to source. By looking at a large number of faint galaxies behind rich clusters, Tyson (1985) found however that the galaxies were preferentially stretched tangentially relative to the cluster centre (if their observed axis ratio is greater than 2, one usually call these "arclets"). Such a distortion is actually what one expects from the lensing effect of the cluster. For a few rich clusters, it has already been possible to estimate their mass from the direct observation and analysis of such arclets. This has only been possible because of the large surface density of faint galaxies that exist everywhere in the sky (about 30 per square arcmin. as reported by Tyson). Furthermore, since these galaxies have different colors (being generally bluer) than those of the cluster members, they can easily be distinguished from the latter ones. Following the success by various theoreticians in fitting gravitational lens models to the observed giant luminous arcs and arclets, it has become clear that the mass responsible for these is characterized by high mass-to-light ratios ($\geq 100 M_\odot / L_\odot$), confirming that at least 90% of the matter is unseen in rich galaxy clusters, in agreement with the values obtained from the somewhat uncertain application of the virial theorem. The studies of arcs and arclets thus provide a new powerful tool for probing the distribution of visible and dark matter

in the Universe. This new type of astrophysical application has been recently reviewed by Tyson (1991).

With the new generation of large format CCDs which will come soon into operation, it should be possible to look for systematic deformation effects of very faint galaxies over large areas of the sky, thereby providing important information on the large scale mass distribution in the Universe.

6.4. Probing the intergalactic medium

Since the light rays associated with the multiply lensed images of a distant quasar have travelled along different lines of sight through the intergalactic medium, it appears very interesting to probe the size and the structure of various types of intergalactic gas clouds by just identifying the number of coincidences and anti-coincidences of narrow absorption lines detected in the spectrum of the multiple QSO images. In doing so, Smette et al. (1992) have reported a study of the Lyα forest on the basis of high resolution spectra obtained at MMTO, ESO and CTIO for the A and B images of the gravitationally lensed high-redshift quasar 0142-100 (cf. Section 5.1.). They have derived a best value of $12 h_{50}^{-1}$ kpc ($q_o = 0$) for the 2 σ lower limit of the diameter of spherical Lyα clouds. Similar studies of other gravitational lens systems (2345+007, see Foltz et al. 1984 and Steidel and Sargent 1991) will enable one to set more stringent constraints on the size of Lyα and heavy element absorption line clouds in the near future.

7. CONCLUSIONS

Just 12 years after their discovery, gravitational lenses constitute today a major field of astronomical research. Theoretical modeling of these enigmatic systems have already provided us with important astrophysical and cosmological information, not attainable in any other way. When looking towards the future, it is also clear that only few fields of astronomy other than gravitational lensing will profit as much from the next generation of large telescopes: for instance, very detailed observations of arcs and arclets will become feasible thanks to the large collecting area of future VLTs, and the study of multiply imaged quasars with small separations will benefit directly from the high angular resolution techniques (speckle imaging, adaptive optics) which are being largely improved. One may therefore feel optimistic about the future of this *very interesting field of research*. Let us finally stress again the great need for a fully dedicated telescope (2-3 m size) for the optical photometric monitoring of quasars, with particular emphasis on the monitoring of multiply imaged sources.

Acknowledgements: We should like to address our thanks to the executive committee of the IAU for having suggested the title of the present talk, and also to the IAU Local Organizing Committee and to Dr. Schmidt (Optical Laboratory from the University of Buenos Aires) for their help in collecting part of the equipment that has been used during the presentation of the optical lens experiment in Buenos Aires. Our thanks go also to Ulf Borgeest, Rolf Stabell and Jean-Pierre Swings for reading the manuscript, to J. Hazlehurst for valuable advice, to J. Arnaud, J. Hewitt, G. Langston, J. Lehár, G. Lelièvre and G. Soucail for providing us with slides of GLs illustrated in Fig. 6, and to J. Bosseloirs and J. Beonkens for the preparation of some of the figures. Part of this research has been supported by the German Research Council (DFG), the Belgian National Research Science Foundation (FNRS) and ARC 90/94-140 "Actions de recherche concertée de la Communauté Française de Belgique".

References:

Angonin, M.C., Remy, M., Surdej, J., Vanderriest, C.: 1990, Astron. Astrophys. Letters 233, L5-L8.

Blandford, R.D., Narayan, R.: 1992, preprint, to appear in Annual Review of Astron. Astrophys.

Borgeest, U.: 1986, Astrophys. J. 309, 467.

Borgeest, U., van Linde, J., Refsdal, S.: 1991, Astron. Astrophys. 251, L35.

Bourassa, R.R., Kantowski, R., Norton, T.D.: 1973, Astrophys. J. 185, 747.

Burke, W.L.: 1981, Astrophys. J. 244, L1.

Chang, K., Refsdal, S.: 1976, Colloques Int. du C.N.R.S., 263, 369.

Chang, K., Refsdal, S.: 1979, Nature 282, 561.

Chwolson, O.: 1924, Astr. Nachr. 221, 329.

Cooke, J.H., Kantowski, R.: 1975, Astrophys. J. 195, L11.

Dyer, C.C., Roeder, R.C.: 1972, Astrophys. J. 174, L115.

Dyson, F.W., Eddington, A.S., Davidson, C.R.: 1920, Phil. Trans. Roy. Soc. 220A, 291; Mem. Roy. Astron. Soc. 62, 291.

Falco, E.E., Gorenstein, M.V., Shapiro, I.I.: 1991, Astrophys. J. 372, 364.

Foltz, C.B., Weymann, R.J., Roeser, H.J., Chaffee, F.H.: 1984, Astrophys. J. 281, L1.

Gorenstein, M.V., Falco, E.E., Shapiro, I.I.: 1988, Astrophys. J. 327, 693.

Grieger, B., Kayser, R., Refsdal, S.: 1986, Nature 324, 126.

Grieger, B., Kayser, R., Refsdal, S.: 1988, Astron. Astrophys. 194, 54.

Hammer, F., Le Fèvre, O.: 1990, Astrophys. J. 357, 38.

Hewitt, J., Turner, E.L., Burke, B.F., Lawrence, C.R., Bennett, C.L., Langston, J.I., Gunn, J.E.: 1987, in "Observational Cosmology", p. 751.

Hewitt, J.N., Turner, E.L., Schneider, D.P., Burke, B.F., Langston, G.I., Lawrence, C.R.: 1988, Nature 333, 537.

Huchra, J., Gorenstein, M., Kent, S., Shapiro, I., Smith, G., Horine, E., Perley, R.: 1985, Astron. J. 90, 691.

Irwin, M.J., Webster, R.L., Hewett, P.C., Corrigan, R.T., Jedrzejewski, R.I.: 1989, Astron. J. 98, 1989.

Kayser, R., Refsdal, S., Stabell, R.: 1986, Astron. Astrophys. 166, 36.

Kayser, R., Refsdal, S.: 1989, Nature 338, 746.

Klimov, Y.G.: 1963, Sov. Phys. Doklady 8, 119.

Kochanek, C.S., Blandford, R.D., Lawrence, C.R., Narayan, R.: 1989, Monthly Notices Roy. Astron. Soc. 238, 43.

Langston, G.I., Schneider, D.P., Conner, S., Carilli, C.L., Lehár, J., Burke, B.F., Turner, E.L., Gunn, J.E., Hewitt, J.N., Schmidt, M.: 1989, Astron. J. 97, 1283.

Lelièvre, G., Nieto, J.-L., Salmon, D.: 1988, Astron. Astrophys. 200, 301.

Liebes, S.: 1964, Phys. Rev. B133, 835.

Lynds, R., Petrosian, V.: 1986, Bull. Am. Astron. Soc. 18, 1014.

Magain, P., Surdej, J., Swings, J.-P., Borgeest, U., Kayser, R., Kühr, H., Refsdal, S., Remy, M.: 1988, Nature 334, 325.

Paczyński, B.: 1986, Astrophys. J. 304, 1.

Paczyński, B.: 1987, Nature 325, 572.

Press, W.H., Gunn, J.E.: 1973, Astrophys. J. 185, 397.

Press, W.H., Rybicki, G.B., Hewitt, J.N.: 1991, CfA preprint 3230.

Refsdal, S.: 1964a, Monthly Notices Roy. Astron. Soc. 128, 295.

Refsdal, S.: 1964b, Monthly Notices Roy. Astron. Soc. 128, 307.

Refsdal, S.: 1965, Proc. of the Int. Conf. on Relativistic Theories of Gravitation, London.

Refsdal, S.: 1966a, Monthly Notices Roy. Astron. Soc. 132, 101.

Refsdal, S.: 1966b, Monthly Notices Roy. Astron. Soc. 134, 315.

Refsdal, S.: 1970, Astrophys. J. 159, 357.

Rhee, G.: 1991, Nature 350, 211.

Schneider, P., Ehlers, J., Falco, E.E.: 1992, "Gravitational Lensing", Springer-Verlag, in press.

Smette, A., Surdej, J., Shaver, P.A., Foltz, C.B., Chaffee, F.H., Weymann, R.J., Williams, R.E., Magain, P.: 1991, Astrophys. J., in press.

Soucail, G., Mellier, Y., Fort, B., Hammer, F., Mathez, G.: 1987, Astron. Astrophys. 184, L7.

Steidel, C.C., Sargent, W.L.W.: 1991, Astron. J., in press.

Surdej, J., Magain, P., Swings, J.-P., Borgeest, U., Courvoisier, T.J.-L., Kayser, R., Kellermann, K.I., Kuhr, H., Refsdal, S.: 1987, Nature 329, 695.

Surdej, J., Swings, J.P., Magain, P., Borgeest, U., Kayser, R., Refsdal, S., Courvoisier, T.J.-L., Kellermann, K.I., Kühr, H.: 1988, in the proceedings of a workshop on "Optical surveys for quasars", Astron. Soc. of the Pac. Conf. Series 2, 183.

Surdej, J., Claeskens, J.F., Hutsemékers, D., Magain, P., Pirenne, B.: 1992, Proc. of the Hamburg Int. Conf. on Gravitational Lenses, Lecture Notes in Physics, Springer-Verlag, in press.

Tyson, J.A.: 1985, Nature 316, 799.

Tyson, J.A.: 1991, preprint.

Vanderriest, C., Gosset, E., Remy, M., Swings, J.P.: 1992, Proc. of the Hamburg Int. Conf. on Gravitational Lenses, Lecture Notes in Physics, Springer-Verlag, in press.

Walsh, D., Carswell, R.F., Weymann, R.J.: 1979, Nature 279, 381.

Wambsganss, J., Paczyński, B., Schneider, P.: 1990, Astrophys. J. 358, L33.

Weymann, R.J., Latham, D., Angel, J.R.P., Green, R.F., Liebert, J.W., Turnshek, D.A., Turnshek, D.E., Tyson, J.A.: 1980, Nature 285, 641.

Zel'dovich, Y.B.: 1964, Soviet Astron. 8, 13.

Zwicky, F.: 1937a, Phys. Rev. Lett. 51, 290.

Zwicky, F.: 1937b, Phys. Rev. Lett. 51, 679.

VOYAGER: A RETROSPECTIVE

Bradford A. Smith
University of Hawaii
Institute for Astronomy
2680 Woodlawn Drive
Honolulu, HI 96822
USA

ABSTRACT. Within the brief span of a decade, from 1979 to 1989, the Voyager spacecraft visited the four giant planets – Jupiter, Saturn, Uranus and Neptune – along with their satellites and their rings. The science return from these two spacecraft forever changed our views of this remote region of our solar system. Often overlooked, however, is the incremental gain in knowledge from these encounters over that which had been known in the early 1970s when the Voyager project first came into being. From a post-Voyager perspective, it is astonishing how little was known about the outer planets just a mere two decades ago. Yet, with all of the knowledge that the space program has brought us, there remain a number of unanswered questions and a great many new ones that have been posed as a result of this wealth of new information. Discussed here is summary of the results of the Voyager imaging cameras together with some of the many new questions that subsequently have been raised.

1. Introduction

It was nearly two decades ago that we, as a community of scientists, reluctantly turned our backs on human exploration of the moon and turned our expectations to the outer solar system. Preparations were then being made to launch two Pioneer spacecraft to Jupiter, and planning was well underway for a "Grand Tour" of the entire outer solar system, making use of a rare planetary alignment that would take place in the year 1977. The fiscal realities of the times, however, soon caused the Grand Tour to be scaled back to a much more modest mission, one that would explore only the two most accessible of the outer planets. On July 1st, 1972, Mariner Jupiter/Saturn, or MJS as it was called, became an approved NASA project, and within six months, even as the Apollo 17 astronauts were bidding a final farewell to the moon, the first of the MJS science planning meetings was already taking place.

Our keen disappointment in the cutback, which might otherwise have dampened those early meetings, was mitigated by the knowledge that *any* spacecraft launched on the right Jupiter-Saturn trajectory in 1977 would also have the capability of continuing onward to both Uranus and Neptune, a fact that may or may not have been understood by the administrative and legislative committees that killed the Grand Tour and substituted MJS. Two identical Mariner-class spacecraft were to be sent to Jupiter and Saturn, and throughout our five years of planning, we carefully held open all options for at least one of them to go beyond. In 1977, just before launch, MJS was renamed Voyager, but it was only *after* launch that the official approval was given to send Voyager 2 onward from Saturn out to Uranus and Neptune.

J. Bergeron (ed.), Highlights of Astronomy, Vol. 9, 33–42.